Journal of Thermal Analysis and Calorimetry, Vol. 87 (2007) 2, 343–348

COMPARATIVE ANALYSIS OF CALORIMETRIC STUDIES IN $Se_{90}M_{10}$ (*M*=In, Te, Sb) CHALCOGENIDE GLASSES

N. Mehta and A. Kumar *

Department of Physics, Harcourt Butler Technological Institute, Kanpur 208 002, India

Calorimetric measurements have been performed in glassy $Se_{90}M_{10}$ (*M*=In, Te, Sb) alloys to study the effect of In, Te and Sb additives on the kinetics of glass transition and crystallization in glassy $Se_{90}M_{10}$ system. Kinetic parameters of glass transition and crystallization such as the activation energy of glass transition (E_g), the activation energy of crystallization (E_c), the order parameter (n), the rate constant (K), etc. have been determined using different non-isothermal methods. The composition dependence of the activation energies of glass transition and crystallization processes is also discussed.

Keywords: *chalcogenide glasses, crystallization kinetics, DSC, glass transition kinetics*

Introduction

There are numerous potential applications of chalcogenide glasses proposed in the civil, medical and military areas [1–6]. It is possible to produce industrially electrical switches, xerographic and thermoplastic media, photo-resistant and holographic media, optical filters, optical sensors, thin films waveguides, non-linear elements, etc. [1–6].

In chalcogenide glasses, Se based glassy alloys belong to an interesting and unique class of amorphous semiconductors and have wide technical applications in electronics and optoelectronics. However, the shortcomings of pure glassy Se for its practical applications include its short lifetime, low sensitivity and thermal instability. To overcome these difficulties, certain additives are used and especially the use of Se–Te, Se–In and Se–Sb binary alloys is of interest owing to their various properties like greater hardness, higher sensitivity, higher conductivity and smaller ageing effects as compared to pure amorphous Se (a-Se).

In case of chalcogenide glasses, the variation in kinetic parameters of glass transition and crystallization on changing the composition in a specific glassy system is studied by various workers. It is interesting to study the kinetics of glass transition and crystallization in a particular ternary glassy system by changing the third element [7, 8]. These days, our lab is engaged in this direction. Recently, the calorimetric studies in glassy $Se_{70}Te_{20}M_{10}$ (*M*=Ag, Cd, Sb) and $Se_{68}Ge_{22}M_{10}$ (*M*=Cd, In, Pb) has been reported by our group [9–12]. In the present paper such systematic calorimetric studies on glassy $Se_{90}M_{10}$ (*M*=In, Te, Sb) alloys has been reported.

Experimental

Materials

Glassy alloys of $Se_{90}M_{10}$ (*M*=In, Te, Sb) were prepared by quenching technique. High purity Se, Te, In and Sb materials (99.999%) were weighed according to their atomic percentages and were sealed in quartz ampoules under the vacuum of 10^{-5} Torr. Each ampoule was kept inside the furnace at 1000°C so that all the elements get melted. The temperature was raised at a rate of 3–4°C min^{-1}. The ampoules were rocked frequently for 12 h at the maximum temperature to make the melt homogeneous. Quenching was done in ice water and the ingots of the samples were taken out by breaking the quartz ampoules.

Methods

The glassy nature of alloys was checked by X-ray diffraction technique. For this, X-ray diffraction (XRD) patterns of all the three samples were taken at room temperature by using an X-ray diffractometer (Philips, PW 1140/09). The copper target was used as a source of X-rays with λ=1.54 Å ($CuK_{\alpha 1}$). The XRD pattern of glassy $Se_{90}Sb_{10}$ is shown in Fig. 1. Absence of any sharp peak in XRD pattern in Fig. 1 confirms the glassy nature of $Se_{90}Sb_{10}$ alloy. Similar XRD patterns were obtained for the other two glassy alloys.

The glasses, thus prepared, were ground to make fine powder for DSC studies. This technique is particularly important due to the facts that: (1) it is easy to carry out; (2) it requires little sample preparation and (3) it is quite sensitive.

* Author for correspondence: dr_ashok_kumar@yahoo.com

1388–6150/$20.00

Akadémiai Kiadó, Budapest, Hungary
Springer, Dordrecht, The Netherlands

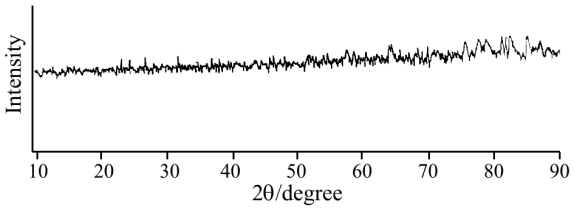

Fig. 1 XRD pattern of glassy $Se_{90}Sb_{10}$ alloy

Before DSC experiment, the thermogravimetric analysis has been made on each glassy sample. Perkin Elmer TGA7 thermogravimetric is used for this purpose. In thermogravimetric analysis, the percent mass loss of a test sample is recorded while the sample is being heated at a uniform rate in an appropriate environment (inert – nitrogen gas). The loss in mass over specific temperature ranges provides an indication of the composition of the sample, including volatiles and inert filler, as well as indications of thermal stability. TG curve for glassy $Se_{90}Sb_{10}$ alloy is shown in Fig. 2, which is a plot of percent mass loss *vs*. temperature. From this figure, it is clear that there is no drastic loss in the mass of the sample over the entire temperature range. Similar TG curves are obtained for the other glassy alloys.

The thermal behaviour was investigated using differential scanning calorimeter (Model-DSC plus, Rheometric Scientific Company, UK). The temperature precision of this equipment is ±0.1 K with an average standard error of about ±1 K in the measured values (glass transition and crystallization temperatures).

10 to 20 mg of each sample was heated at a constant heating rate and the changes in heat flow with respect to an empty pan were measured. Four heating rates (5, 10, 15 and 20°C min^{-1}) were chosen in the present study. Measurements were made under almost identical conditions.

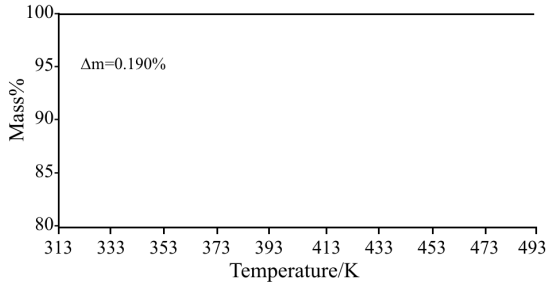

Fig. 2 TG curve for glassy $Se_{90}Sb_{10}$ alloy

Results and discussion

Figure 3 shows DSC curves at different heating for $Se_{90}Sb_{10}$ alloys. It is clear from Fig. 3 that well defined endothermic peaks are observed at the glass transition temperature T_g. The well defined exothermic peaks are obtained at the crystallization temperature T_c. Similar curves have been obtained for the other glassy alloys. The values of T_g and T_c at different heating rates for the various glassy alloys are given in Table 1.

Table 1 Values of T_g and T_c (in K) for glassy $Se_{90}M_{10}$ alloys at different heating rates

Heating rate/ K min^{-1}	$Se_{90}In_{10}$		$Se_{90}Te_{10}$		$Se_{90}Sb_{10}$	
	T_g	T_c	T_g	T_c	T_g	T_c
5	335	378	328	390	325	381
10	344	387	331	395	327	389
15	350	392	333	399	328	395
20	354	397	335	403	329	399

Glass transition kinetics and kinetic parameters of glass transition

Two approaches are used in the analysis of the dependence of T_g on the heating rate. The first is the empirical relation that has been suggested by Lasocka [13] and has the form:

$$T_g = A + B\log\beta \quad (1)$$

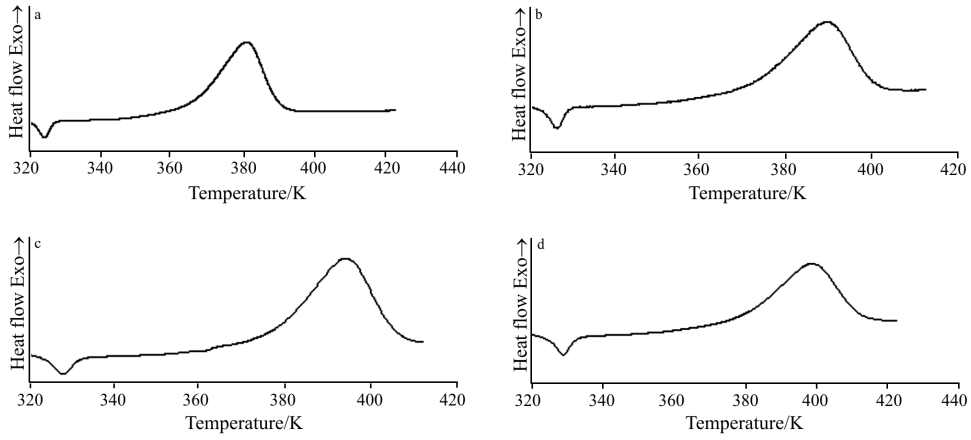

Fig. 3 DSC curves for glassy $Se_{90}Sb_{10}$ alloy at different heating rates; a – 5, b – 10, c – 15 and d – 20 K min^{-1}

Table 2 Kinetic parameters of glass transition and crystallization for glassy $Se_{90}M_{10}$ alloys

Sample	E_g/kJ mol^{-1}		A/K	B/min	E_c/kJ mol^{-1}		
	Eq. (2)	Eq. (3)			Eq. (5)	Eq. (8)	Eq. (9)
$Se_{90}In_{10}$	65.8	71.5	312.7	31.6	92.3	89.0	85.8
$Se_{90}Te_{10}$	177.4	182.8	319.9	11.4	139.9	136.6	133.3
$Se_{90}Sb_{10}$	248.6	253.4	319.0	8.0	97.0	93.8	90.6

where A and B are constants. The values of A and B for different alloys are given in Table 2. The results shown in Table 2 indicate the validity of this relationship for the various alloys. The plots of T_g *vs*. logβ for all glassy alloys are shown in Fig. 4. The value of A indicates the glass transition temperature for the heating rate of 1 K min^{-1}. It has been found by the various workers that the slope B in the Eq. (1) is related to the cooling rate of the melt: the lower the cooling rate of the melt, the lower the value of B. The physical significance of B seems to be related with the response of the configurational changes within the glass transformation region. The values of B for various alloys have been found to be different, indicating that these glassy alloys undergo different structural changes.

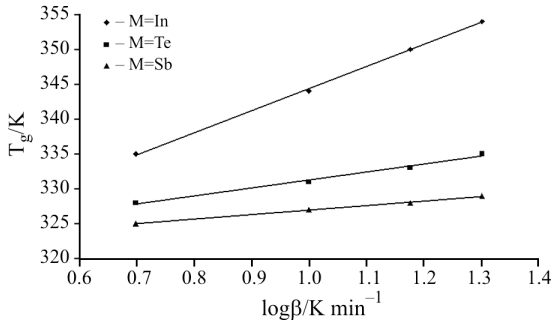

Fig. 4 Plots of T_g *vs*. logβ for glassy $Se_{90}M_{10}$ alloys

The second approach concerns the use of the Kissinger's linear dependence [14] in the form:

$$\ln(\beta/T_g^2)=E_g/RT_g+\text{constant} \quad (2)$$

In addition, when the variation of $\ln(1/T_g^2)$ with lnβ is much slower than that of $1/T_g$ then Eq. (2) converts in to the form [15]:

$$\ln\beta=-E_g/RT_g+\text{constant} \quad (3)$$

The plots of $\ln(\beta/T_g^2)$ and lnβ *vs*. $10^3/T_g$ for all glassy alloys are shown in Fig. 5. Using the slopes of these plots, the activation energy of the glass transition process is calculated for the various alloys and is given in Table 2. It is clear from this table that the E_g values are in good agreement with each other. This shows that one can use any of the Eqs (2) and (3) for the evaluation of E_g.

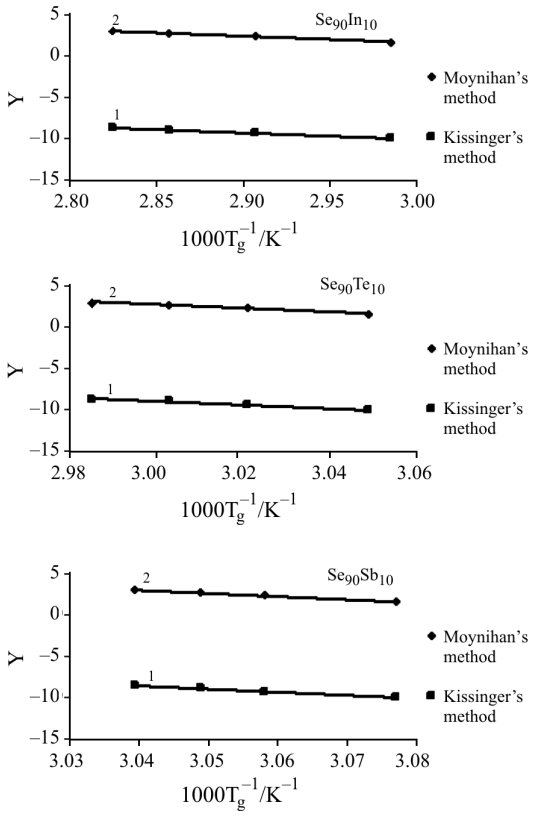

Fig. 5 Plots of 1 – $\ln\beta/T_g^2$ and 2 – lnβ *vs*. $10^3/T_g$ for glassy $Se_{90}M_{10}$ alloys

In order to evaluate the stability in glasses, Hu *et al*. [16] developed $K(T_c)$ criterion:

$$K(T_c)=K_0\exp[-E_c/(RT_c)] \quad (4)$$

The values of this stability criterion for glassy $Se_{90}M_{10}$ (M=In, Te, Sb) alloys are given in Table 3.

Table 3 Values of $K(T_c)$ for glassy $Se_{90}M_{10}$ alloys at different heating rates

Heating rate/ K min^{-1}	$Se_{90}In_{10}$	$Se_{90}Te_{10}$	$Se_{90}Sb_{10}$
5	$1.19\cdot10^{-11}$	$1.87\cdot10^{-17}$	$1.66\cdot10^{-44}$
10	$2.30\cdot10^{-11}$	$3.19\cdot10^{-17}$	$2.49\cdot10^{-41}$
15	$3.27\cdot10^{-11}$	$4.85\cdot10^{-17}$	$2.25\cdot10^{-39}$
20	$4.62\cdot10^{-11}$	$7.30\cdot10^{-17}$	$4.79\cdot10^{-38}$

Crystallization kinetics and kinetic parameters of crystallization

Based on JMA model [17–19], different authors have developed very diverse methods for the evaluation of the activation energy of crystallization (E_c) of the chalcogenide glasses.

According to Kissinger [14], the peak crystallization temperature T_c, in terms of the heating rate β, can be expressed as:

$$\ln(\beta/T_c^2)=-E_c/RT_c+\text{constant} \quad (5)$$

This equation is used to calculate the activation energy of crystallization by plotting $\ln\beta/T_c^2$ *vs*. $10^3/T_c$ curve.

The extent of crystallization (α) at a temperature T is well expressed by the expression:

$$\ln(1-\alpha)^{-1}=(C/\beta^n)[(-nE_c)/RT] \quad (6)$$

derived by Matusita and Sakka [20, 21] from the classical JMA equation. For constant temperature, this equation can be written as:

$$\ln[\ln(1-\alpha)^{-1}]=-n\ln\beta+\text{constant} \quad (7)$$

From this equation, the value of n can be calculated by plotting $\ln[\ln(1-\alpha)^{-1}]$ *vs*. lnβ curves at different temperatures.

Further, since the values of α are independent of β at $T=T_c$ [22], so at $T=T_c$, Eq. (6) takes the form:

$$\ln\beta=-E_c/RT_c+\text{constant} \quad (8)$$

This equation is used to calculate the activation energy of crystallization by plotting lnβ *vs*. $10^3/T_c$ curve.

The activation energy of crystallization E_c can also be determined by an approximation method developed by Augis and Bennett [23]. The relation used by them is of the form:

$$\ln\beta/T_c=-E_c/RT_c+\ln K_0 \quad (9)$$

The activation energy of crystallization can be evaluated by this equation using the plots of $\ln\beta/T_c$ *vs*. $10^3/T_c$. This method has an extra advantage that the intercept of $\ln\beta/T_c$ *vs*. $1/T_c$ gives the value of pre-exponential factor K_0 of Arrhenius equation.

The plots of $\ln(\beta/T_c^2)$, lnβ and $\ln(\beta/T_c)$ *vs*. $10^3/T_c$ for all glassy alloys are shown in Fig. 6. Using the slopes of these plots, the activation energy of the crystallization process is calculated for the various alloys and is given in Table 2. It is clear from this table that the E_c values are in good agreement with each other. This shows that one can use any of the Eqs (5), (8) and (9) for the evaluation of E_c.

The fraction 'α' crystallized at any temperature T is given as $\alpha=A_T/A$, where A is the total area of the exothermic peak between the temperature T_b where the peak begins (i.e. the crystallization starts) and the

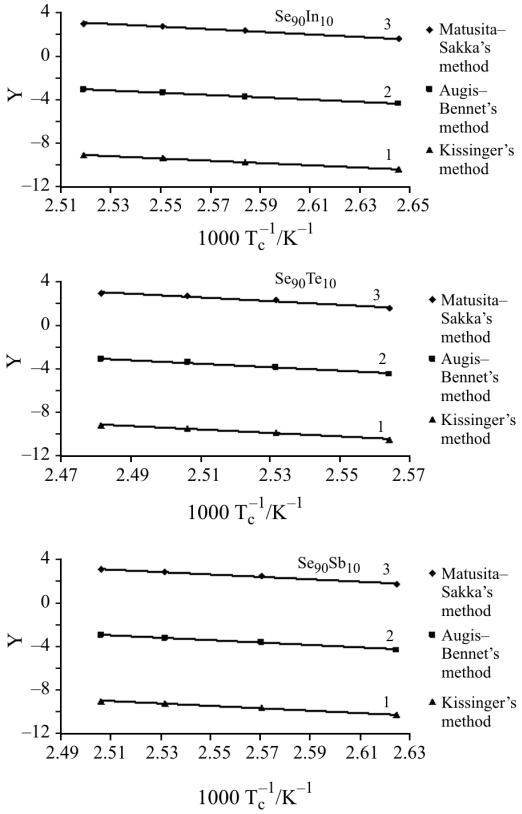

Fig. 6 Plots of 1 – $\ln\beta/T_c^2$, 2 – $\ln\beta/T_c$ and 3 – lnβ *vs*. $10^3/T_c$ for glassy $Se_{90}M_{10}$ alloys

temperature T_e where the peak ends (i.e. the crystallization is complete). A_T is the partial area of the exothermic peak between the temperatures T_b and T. Using Eq. (7), the values of n have been determined at different temperatures for all the glassy alloys. The plots of $\ln[\ln(1-\alpha)^{-1}]$ *vs*. lnβ are shown in Fig. 7 for glassy $Se_{90}Te_{10}$ alloy at three different temperatures. Similar plots were obtained for the other two glassy alloys. The values of Avrami index '*n*' at three different temperatures are given in Table 4. Since the as-quenched samples are studied, the dimensionality of growth m is taken as $m=n-1$ [24]. The values of m are also listed in Table 4. From Table 4, it is clear that m is unity for all the samples, indicating a two-dimensional growth in glassy $Se_{90}M_{10}$ alloys.

When the liquid is cooled in the glass transition region, the relaxation times for molecular movements become comparable to the experimental time scale.

Table 4 Temperature dependence of Avrami index *n*

$Se_{90}In_{10}$			$Se_{90}Te_{10}$			$Se_{90}Sb_{10}$		
T/K	*n*	*m*	*T*/K	*n*	*m*	*T*/K	*n*	*m*
278.0	2.23	1	273.0	2.15	1	389.5	2.26	1
283.0	2.00	1	278.0	2.00	1	391.5	2.10	1
288.0	1.85	1	283.0	1.95	1	393.5	1.90	1

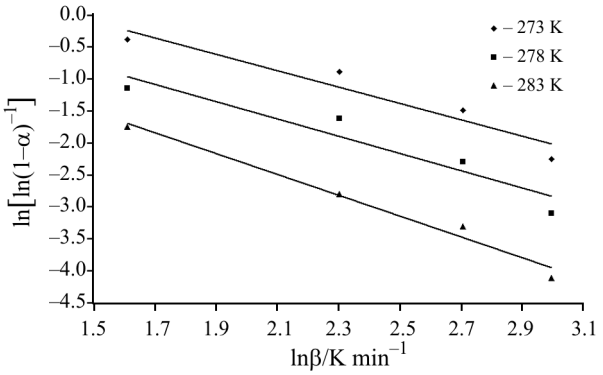

Fig. 7 Plots of $\ln[\ln(1-\alpha)^{-1}]$ *vs*. $\ln\beta$ for glassy $Se_{90}Te_{10}$ alloy at different temperatures

Therefore, the diffusive movements become comparable to the experimental time scale. Therefore, the diffusive motion of the liquid is trapped and the system falls out of thermal equilibrium [25]. At this moment, the size of the nuclei does not reach the critical size required to initiate the nucleation process and hence the glass is assumed to have no nuclei (of critical size). According to Matusita *et al*. [24], when the glass is heated in the DSC furnace, the rate of crystal nucleation in glass reaches the maximum at a temperature somewhat higher than the glass transition temperature and then decreases rapidly with increasing temperature, while the rate of crystal growth reaches the maximum at a temperature much higher than the temperature at which the nucleation rate is highest. When the glass is heated at a constant rate, the crystal nuclei are formed only at lower temperatures and crystal grow in size at higher temperatures without any increase in number of nuclei.

From Table 4, it is clear that '*n*' decreases with increase in temperature. It is well known that crystallization of chalcogenide glasses is associated with nucleation and growth process and the extent of crystallization α increases with increase in temperature. In other words it tends to its maximum value 1. The decrease in order parameter with increasing temperature for glassy $Se_{90}M_{10}$ alloys suggests that the character of crystallization goes over from nucleation-driven in the beginning to essentially a growth-driven regime by the end of crystallization process.

Composition dependence of E_g

The glass transition activation energy is that amount of energy, which is absorbed by a group of atoms in the glassy region so that a jump from one metastable state to another is possible. This means that E_g is involved in the molecular motions and rearrangements of atoms in the glass transition region. When the sample is heated in DSC furnace, the atoms undergo infrequent transitions between the local potential minima separated by different energy barriers in the configuration space, where each local minimum represents a different structure. The most stable local minimum in the glassy region has lower internal energy. Accordingly, the atoms in the glass having minimum activation energy have higher probability to jump to the metastable state (or local minimum) state of lower internal energy and hence are the most stable. In the glassy $Se_{90}M_{10}$ (*M*=In, Te, Sb) alloys, E_g increases in the sequence $(E_g)_{In}<(E_g)_{Te}<(E_g)_{Sb}$, which indicates that thermal stability of glassy $Se_{90}M_{10}$ system is increased in the sequence $(Se_{90}Sb_{10})<(Se_{90}Te_{10})<(Se_{90}In_{10})$. This is also confirmed from the values of $K(T_c)$ for the present alloys, which increases in the sequence $[K(T_c)]_{Sb}<[K(T_c)]_{Te}<[K(T_c)]_{In}$. Hence one can conclude that the activation energy of glass transition process is related to thermal stability. Higher thermal stability may require less activation energy for glass transition process as found in the present study.

Composition dependence of E_c

From Table 2, it is clear that the value of E_c in $Se_{90}M_{10}$ system increases in the sequence. $(E_c)_{In}<(E_c)_{Sb}<(E_c)_{Te}$. This sequence can be explained to some extent in terms of average heat of atomization for these alloys. The average heat of atomization H_S, is based on chemical bonding aspects, is defined for an alloy X_aY_b as a direct measure of cohesive energy i.e., of the average bond strength [26]. H_S can be given as:

$$H_S=[a(H_S)_X+b(H_S)_Y]/(a+b) \qquad (10)$$

where $(H_S)_X$ and $(H_S)_Y$ are the heat of atomization of atoms X and Y, respectively. The average heat of atomization H_S for Se, Te, In and Sb are taken from [27]. The value of H_S for $Se_{90}M_{10}$ system (*M*=In, Te, Sb) are given in Table 5.

Table 5 The average bond strength of glassy $Se_{90}M_{10}$ alloys

Sample	H_S/kJ mol^{-1}
$Se_{90}In_{10}$	209.3
$Se_{90}Te_{10}$	224.0
$Se_{90}Sb_{10}$	221.8

The average bond strength of glassy $Se_{90}M_{10}$ (*M*=In, Te, Sb) alloys increases in the sequence $(H_S)_{In}<(H_S)_{Sb}<(H_S)_{Te}$. This shows that higher the average bond strength of the binary alloy, more is the activation energy of crystallization. The plot of E_c *vs*. H_S is shown in Fig. 8.

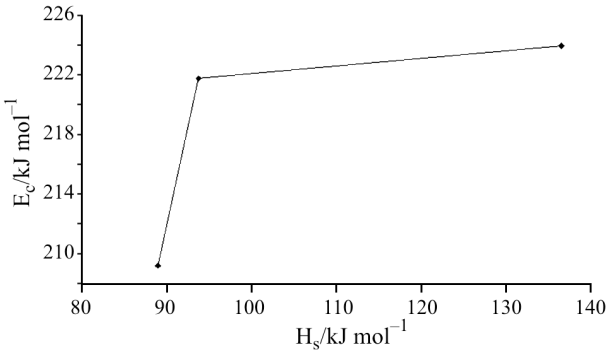

Fig. 8 Plot of activation energy of crystallization E_c *vs*. average bond strength H_S

Conclusions

The kinetics of glass transition and crystallization in glassy $Se_{90}M_{10}$ (M=In, Te, Sb) alloys have been studied by non-isothermal DSC technique. The activation energies of the glass transition and crystallization processes for these chalcogenide glasses have been calculated using the different non-isothermal methods.

The activation energy of glass transition process (E_g) is found to be related with stability criteria based on Arrhenius dependence of rate constant K in reverse sequence. Hence one can conclude that the activation energy of glass transition process is related to thermal stability in the present glasses and the chalcogenide glasses having higher activation energy for glass transition process shows less thermal stability. The composition dependence of activation energy of crystallization in $Se_{90}M_{10}$ system is explained in terms of average heat of atomization for these alloys.

References

1 T. Ohta, J. Optoelectron. Adv. Mater., 3 (2001) 609.
2 A. M. Andriesh, M. S. Iovu and S. D. Shutov, J. Optoelectron. Adv. Mater., 4 (2002) 631.
3 A. V. Kolobov and J. Tominaga, J. Optoelectron. Adv. Mater., 4 (2002) 679.
4 A. Zakery and S. R. Elliott, J. Non-Cryst. Solids, 330 (2003) 1.
5 D. Lezal, J. Optoelectron. Adv. Mater., 5 (2003) 23.
6 B. Bureau, X. H. Zhang, F. Smektala, J.-L. Adam, J. Troles, H.-L. Ma, C. Boussard-Pledel, J. Lucas, P. Lucas, D. Le Coq, M. R. Riley and J. H. Simmons, J. Non-Cryst. Solids, 354 and 346 (2004) 276.
7 M. A. Mousa and M. A. Ahmed, J. Non-Cryst. Growth, 88 (1988) 411.
8 M. B. El-Den, Egypt. J. Sol., 24 (2001) 171.
9 N. Mehta and A. Kumar, J. Mater. Sci., 39 (2004) 6433.
10 N. Mehta, R. K. Shukla and A. Kumar, J. Optoelectron. Adv. Mater., 6 (2004) 1185
11 R. S. Tiwari, N. Mehta, P. Agarwal, R. K. Shukla and A. Kumar, Indian J. Pure Appl. Phys., 43 (2005) 363.
12 N. Mehta, P. Agarwal and A. Kumar, Turkish J. Phys., 29 (2005) 193.
13 M. Lasocka, Mater. Sci. Eng., 23 (1976) 173.
14 H. E. Kissinger, Anal. Chem., 29 (1957) 1702.
15 S. Mahadevan, A. Giradhar and A.K. Singh, J. Non-Cryst. Solids, 88 (1986) 11.
16 L. Hu and Z. Jiang, J. Chin. Ceram. Soc., 18 (1990) 315.
17 W. A. Johnson and R. F. Mehl, Trans. Am. Inst. Min. (Metal) Engs., 135 (1939) 416.
18 M. Avrami, J. Phys. Chem., 7 (1939) 1103.
19 M. Avrami, J. Phys. Chem., 8 (1940) 212.
20 K. Matusita and S. Sakka, Phys. Chem. Glasses, 20 (1979) 81.
21 K. Matusita and S. Sakka, Bull. Inst. Chem. Res. Kyoto Univ., 59 (1981) 159.
22 T. Ozawa, J. Thermal Anal., 2 (1970) 301.
23 J. A. Augis and J. E. Bennett, J. Thermal Anal., 13 (1978) 283.
24 K. Matusita, T. Konatsu and R. Yokota, J. Mater. Sci., 19 (1984) 291.
25 M. M. A. Imran, N. S. Saxena, D. Bhandari and M. Zulfequar, Phys. Stat. Sol. A, 181 (2000) 357.
26 M. Yamaguchi, Philos. Mag., 51 (1985) 651.
27 M. H. R. Lankhorst, J. Non-Cryst. Solids, 297 (2002) 210.

Received: October 25, 2005
Accepted: July 21, 2006

DOI: 10.1007/s10973-005-7411-3